Insight into the removal and reapplication of small inhibitor molecules during area-selective atomic layer deposition of SiO2

JVST A
Journal of Vacuum Science & Technology A

ARTICLE

avs.scitation.org/journal/jva

Insight into the removal and reapplication of small inhibitor molecules during area-selective atomic layer deposition of SiO_2

Cite as: J. Vac. Sci. Technol. A 39, 012402 (2021); doi: 10.1116/6.0000652
Submitted: 20 September 2020 · Accepted: 9 November 2020 ·
Published Online: 4 December 2020

Marc J. M. Merkx,[1] Rick G. J. Jongen,[1] Alfredo Mameli,[1,a)] Paul C. Lemaire,[2] Kashish Sharma,[2] Dennis M. Hausmann,[2] Wilhelmus M. M. Kessels,[1] and Adriaan J. M. Mackus[1]

AFFILIATIONS

[1]Department of Applied Physics, Eindhoven University of Technology, Eindhoven 5600MB, The Netherlands
[2]Lam Research Corporation, Portland, Oregon 97062

Note: This paper is a part of the Special Topic Collection on Area Selective Deposition.
[a)]**Present address:** TNO-Holst Centre, High Tech Campus 31, 5656 AE Eindhoven, The Netherlands

ABSTRACT

As the semiconductor industry progresses toward more complex multilayered devices with ever smaller features, accurately aligning these layers with respect to each other has become a bottleneck in the advancement to smaller transistor nodes. To avoid alignment issues, area-selective atomic layer deposition (ALD) can be employed to deposit material in a self-aligned fashion. Previously, we demonstrated area-selective ALD of SiO_2 using three-step (i.e., ABC-type) ALD cycles comprising an acetylacetone (Hacac) dose (step A), a bis(diethylamino)silane precursor dose (step B), and an O_2 plasma exposure (step C). In this work, the mechanisms of the removal and reapplication of the inhibitor molecules during area-selective ALD were studied, with the aim of enhancing the selectivity of the process. *In situ* infrared spectroscopy shows that the O_2 plasma exposure does not completely remove the adsorbed Hacac species (i.e., acac adsorbates) at the end of the cycle. The persisting species were found to contain fragments of Hacac molecules, which hinder subsequent inhibitor adsorption in the next ALD cycle, and thereby contribute to a loss in selectivity. Alternatively, it was found that an H_2 plasma is able to completely remove all acac species from the surface. An improvement in selectivity was achieved by using a four-step ALD cycle that includes an H_2 plasma step, allowing the nucleation delay to be prolonged from 18 ± 2 to 30 ± 3 ALD cycles. As a result, 2.7 ± 0.3 nm SiO_2 can be deposited with a selectivity of 0.9, whereas only 1.6 ± 0.2 nm can be achieved without the H_2 plasma step. This work shows that the addition of a dedicated inhibitor removal step before the reapplication of the inhibitors can significantly improve the selectivity.

I. INTRODUCTION

Feature alignment in complex multilayered devices is becoming a major bottleneck for the fabrication of nanoelectronics at sub-5 nm nodes.[1–3] Self-aligned fabrication schemes are currently being developed to relax these constraints.[2–7] To enable the development of self-aligned fabrication schemes, bottom-up processing steps are needed in which material is only deposited where it is required, referred to as area-selective deposition (ASD). ASD exploits differences in local surface chemistry on a patterned substrate to allow for selective deposition of a material. Since ASD employs the pattern on a substrate as a template, the deposited material is intrinsically aligned to the initial pattern.

Atomic layer deposition (ALD) relies on the alternating, self-limiting adsorption of a precursor and a coreactant.[8] ALD provides a high uniformity, conformality, and atomic-level thickness control, which, when combined with the self-alignment of ASD, yields a bottom-up process with a high control of the material deposition. ALD typically results in uniform deposition of material over the entire substrate. In some specific cases, the selective adsorption of an ALD precursor can be exploited to achieve ASD;[9–11] however, in general, the process needs to be altered to enable area-selective ALD. For example, the non-growth area (i.e., the surface on which no deposition should take place) can be deactivated by selective functionalization using inhibitor molecules such that precursor

adsorption only takes place on the growth area (i.e., the surface on which deposition is desired).

Self-assembled monolayers (SAMs) are often used as inhibitor layers, which are typically applied prior to ALD using wet chemistry.[12–18] Alternatively, small inhibitor molecules are recently being considered for deactivation of the non-growth area.[19–22] Here, we consider small inhibitor molecules that can be applied in vapor phase during the area-selective ALD process. In general, the selectivity of an area-selective ALD process is eventually lost after a certain number of ALD cycles, through degradation of the inhibitor layer, e.g., by thermal desorption of the inhibitor, interactions between the inhibitor and the precursor, or the use of highly reactive coreactants like ozone or plasmas.[21,23–25] As a result, reapplication of the inhibitors can greatly benefit the selectivity.[26] Selectivity is typically defined as $S = \frac{\theta_{ga} - \theta_{nga}}{\theta_{ga} + \theta_{nga}}$, where θ_{ga} and θ_{nga} correspond to the amounts of deposited material on the growth area and on the non-growth area, respectively.[27]

Our approach to area-selective ALD relies on vapor-phase reapplication of small inhibitor molecules at the start of every ALD cycle as illustrated in Fig. 1. Vapor-phase dosing is desired in industrial processing, since it allows for application of the inhibitor in much shorter time scales and in the same vacuum vessel as used for the ALD process. By using small inhibitor molecules, we previously demonstrated area-selective ALD of SiO_2, WS_2, and TiN.[20,21,28,29] In this approach, the inhibitor molecules are only required to remain on the surface until the end of the subsequent precursor dose. As a result, degradation of the inhibitor layer plays a much smaller role in the selectivity of the process, when compared to approaches that involve surface functionalization only before the deposition. Moreover, this approach is compatible with the use of a plasma as the coreactant.

Area-selective ALD of SiO_2 is of interest since SiO_2 is commonly used as a low-κ insulation material in the semiconductor industry.[30] An important application of area-selective SiO_2 ALD is the fabrication of a fully self-aligned vertical interconnect access (FSAV with V is via). Recently, it became clear that the FSAV will most likely pioneer area-selective ALD in the industry.[4,6] This application aims at relaxing the alignment constraints for lower-level metal interconnects (i.e., M1 and M2 metal layers) in the back-end-of-line (BEOL) by selectively depositing a low-κ dielectric (e.g., SiO_2) on the dielectric surfaces in between the metal lines.[2,3,5] The material added by area-selective deposition creates a topography that mitigates the consequences of alignment errors in the subsequent via fabrication. The thickness of the dielectric that forms this topography only needs to be a few nanometers depending on the quality and choice of the dielectric material.[4] It is challenging to perform thermal ALD of SiO_2 at low substrate temperatures due to the low reactivity that Si precursors have toward either the surface or the coreactant, and SiO_2 is, therefore, typically deposited using plasma-assisted ALD.[31,32] As a result, processes for area-selective ALD of SiO_2 are required to be compatible with a plasma as the coreactant.

To enable area-selective ALD of SiO_2, we previously demonstrated a process that employs ABC-type ALD cycles comprising the dosing of acetylacetone (Hacac) inhibitor molecules (step A), bis(diethylamino)silane (BDEAS) precursor molecules, and an oxygen plasma exposure (step C).[20,21] In our previous work, we have investigated the blocking of precursor molecules by adsorbed Hacac inhibitor molecules and found that Hacac adsorbs in two different bonding configurations, i.e., chelate and monodentate configuration.[21] Hacac adsorbates in monodentate configuration are unable to block BDEAS precursor adsorption, which leads to a loss in selectivity. Therefore, besides the main requirements for an inhibitor molecule in terms of selective adsorption and good precursor blocking, all possible inhibitor adsorption configurations need to be considered when selecting suitable inhibitor molecules for area-selective ALD. In addition, the use of a plasma coreactant

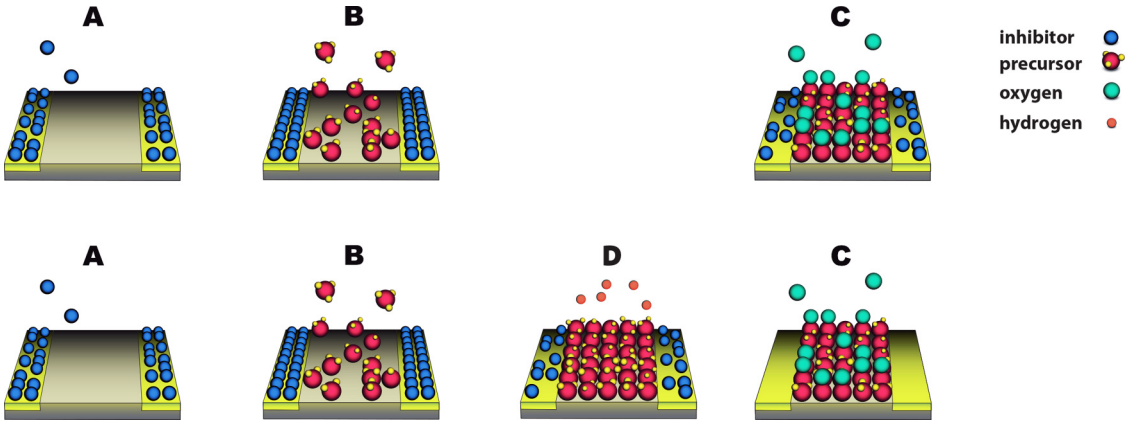

FIG. 1. Schematic illustration of the original ABC-type ALD cycle and the improved ABDC-type ALD cycle for area-selective ALD of SiO_2. In the original process, inhibitor molecules are dosed during step A, which selectively adsorb on the non-growth area of a pattern. Subsequently, the adsorbed inhibitor molecules block precursor adsorption on the non-growth area during step B when the precursor is dosed. Finally, in step C, the inhibitor molecules and the precursor ligands are (partially) removed from the surface by an O_2 plasma exposure. The improved process includes an additional step (step D) prior to the O_2 plasma during which the substrate is exposed to an H_2 plasma. During this step, the inhibitor molecules are more effectively removed from the non-growth area.

during area-selective ALD introduces requirements for the process concerning the inhibitor removal and reapplication, which have to be satisfied independently from the requirements identified in our previous work. During a plasma exposure, a large portion of the inhibitor molecules are expected to be removed from the non-growth area, and it is therefore critical that reapplication of the inhibitor molecules restores the inhibitor layer to its original state before the plasma exposure. In order to prevent the formation of defects in the inhibitor layer as a result of repeated removal and reapplication of inhibitors [see Fig. 2(a)], the coreactant must completely remove the inhibitor adsorbates from the surfaces or alternatively should not induce dissociation of the inhibitor species. The latter is very challenging to achieve when using organic molecules as inhibitors. Therefore, complete inhibitor removal during every cycle should be targeted to achieve high selectivity.

The aim of this work is to provide insight into the reaction mechanisms involved in the cycle-wise removal and reapplication of small inhibitor molecules during area-selective ALD. To this end, inhibitor adsorption and plasma removal were studied using *in situ* ellipsometry and infrared (IR) spectroscopy, considering Hacac on an Al_2O_3 non-growth area as a model system. It was found that an O_2 plasma is unable to completely remove the inhibitor species from the non-growth area, which leads to loss of selectivity. Therefore, the addition of an H_2 plasma step in a four-step process (see Fig. 1) was studied in order to more effectively remove Hacac inhibitor species from the surface. The nucleation behavior of the ALD processes and the impurity levels of the SiO_2 films deposited with and without H_2 plasma steps were investigated. Based on the acquired insights, the process requirements for the removal and reapplication of inhibitor molecules are discussed.

II. EXPERIMENTAL DETAILS

A. Reactors

The IR experiments were performed in a home-built ALD reactor. This reactor is equipped with an inductively coupled plasma source, a turbo-molecular pump backed by a roughing pump, and a Prevac manipulator as described in more detail in a previous work.[21] All other depositions were performed in an Oxford Instruments FlexAL reactor, which is similar to the home-built reactor in terms of the plasma source and pump system but is also equipped with a loadlock.[33]

B. ALD process

The three-step (i.e., ABC-type) ALD process employed in this work is identical to the ABC-type process described in our previous work.[20,21] For the four-step (i.e., ABDC-type) ALD process, 4 s H_2 gas flow stabilization, 25 s H_2 plasma, and 3 s purge steps were added between the precursor and O_2 plasma step without alteration of the rest of the cycle (Fig. 1). All plasma exposures in this work were operated with a grounded substrate table. The H_2 plasma was operated at 300 mTorr and 600 W. These plasma conditions were found to yield optimal results in terms of the selectivity (see Fig. S1 in the supplementary material[46]). Before each deposition, the substrate was exposed to Ar (100 SCCM) and O_2 (50 SCCM) flows at 250 mTorr for 20 min to facilitate the heating of the substrate to a stable temperature. Subsequently, the substrate was exposed to 5 min of O_2 plasma in order to remove any adventitious carbon from the surface. All experiments were performed at 150 °C.

C. IR spectroscopy

The details of the IR setup are described in a previous work.[21] Instead of a powder substrate, a planar Si substrate was employed, which prevents surface recombination of plasma radicals from affecting the experimental results. The sample was heated by an electrical current through the Si substrate, and the temperature was monitored using a thermocouple that was attached to the substrate. Prior to the experiments, these substrates were coated using 30 ALD cycles of the Al_2O_3 (TMA/H_2O) ALD process at 300 °C.

D. Spectroscopic ellipsometry

The subcycle results of Fig. 2 and the nucleation curves in Fig. 6 were measured using *in situ* spectroscopic ellipsometry. A J.A. Woollam M2000D ellipsometer with a range of 1.3–5 eV was employed at an angle of incidence of 70°. All ellipsometry experiments were performed on planar substrates in the Flexal reactor. For the subcycle experiments, alternating Hacac and plasma exposures were applied to the substrate, and ellipsometry measurements were performed after each exposure. These experiments allow for investigating the amount of added and removed inhibitor species after each individual step. Since the dielectric function of a monolayer of adsorbed Hacac is unknown, the ellipsometry measurements yield an "apparent" thickness, which can be used as a measure of adsorbed inhibitor molecules on the surface.[34] To determine the nucleation curves presented in Fig. 6, ellipsometry measurements were only performed at the end of each ALD cycle and give insight into how much SiO_2 has been deposited on the substrate. A Cauchy model (A = 1.55, B = 0.01; n = 1.58 at 600 nm) was used to determine the adsorption of Hacac (Fig. 2) and the growth of SiO_2 (Fig. 6). Prior to the experiments, the substrates were coated with either Al_2O_3 or SiO_2 using 300 ALD cycles of TMA/O_2 plasma or BDEAS/O_2 plasma, respectively.

E. X-ray photoelectron spectroscopy

The XPS depth profiles were measured using a K-Alpha system from Thermo Scientific. A 1000 eV Ar ion beam was employed to sputter through a 10 nm SiO_2 film. Sputter intervals of 30 s were used between measurements. A distinction was made between elemental Si (99.4 eV) and SiO_2 (103.5 eV) in the Si 2p peak in order to differentiate between the substrate and the deposited film. Before depth profiling, a survey measurement was performed over the entire range of the XPS (0–1350 eV) to rule out any unexpected impurities.

III. RESULTS AND DISCUSSION

Subcycle ellipsometry measurements were performed in order to study the removal and reapplication of inhibitor species when using a plasma as the coreactant. As discussed in the Introduction, all adsorbed inhibitor species should be removed from the surface after the plasma exposure to ensure a clean non-growth area for the subsequent ALD cycle [Fig. 2(a)]. However, the ellipsometry results in Fig. 2(b) indicate that the removal of acac species from an Al_2O_3 substrate using O_2 plasma is incomplete, because the apparent

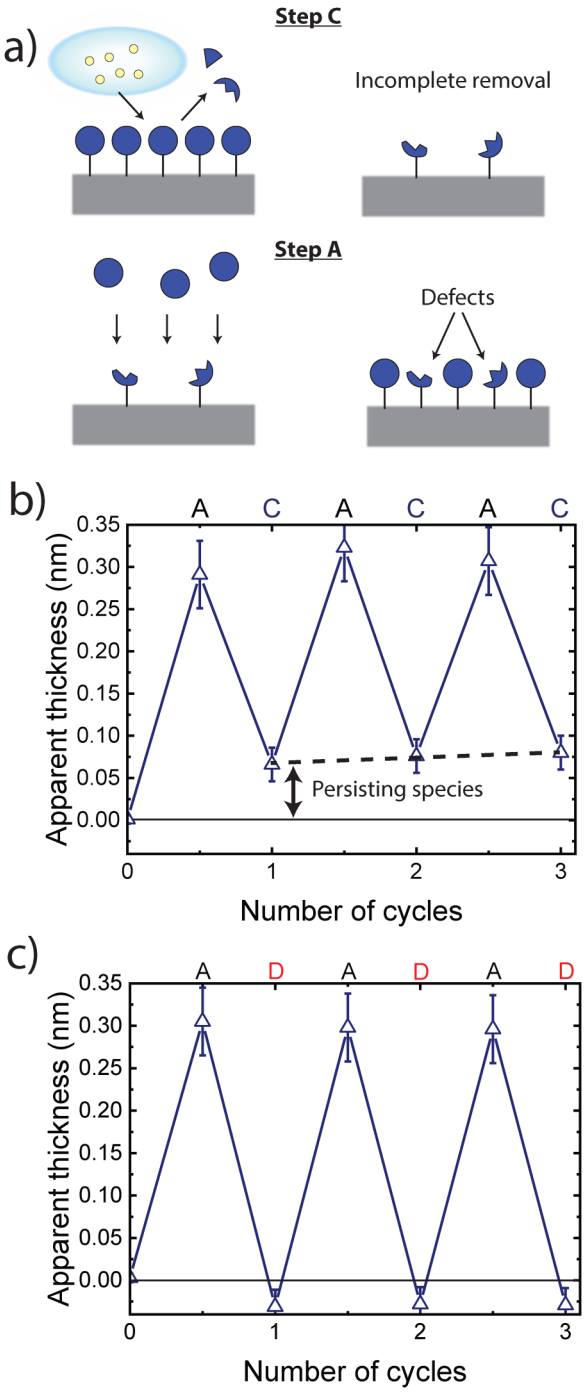

FIG. 2. Removal of Hacac inhibitor species using a plasma. (a) Schematic illustration of how incomplete removal of inhibitor species leads to defects in the inhibitor layer. During the plasma exposure, the inhibitor is incompletely removed leaving fragments on the surface. These fragments could hinder inhibitor adsorption in the next cycle and do not necessarily block precursor adsorption equally well as intact molecules, therefore leading to a loss of selectivity. (b) and (c) Subcycle ellipsometry results showing the apparent thickness of Hacac inhibitor species adsorbed on an Al_2O_3 substrate during alternating (b) Hacac (step A) and O_2 plasma (step C) pulses or (c) Hacac and H_2 plasma (step D) pulses. Since the dielectric function of a layer of acac adsorbates is unknown, a simple Cauchy model was used to determine the apparent thickness of the inhibitor layer. This apparent thickness does not correspond to the actual thickness of the inhibitor layer but can be used as a measure of the adsorbed inhibitor species on the surface.[34] The results show that there are persisting inhibitor species on the surface after the O_2 plasma exposures, whereas the inhibitor species appear to be completely removed after the H_2 plasma exposures.

thickness does not return to 0 nm. After each Hacac dose, the apparent thickness returns to approximately the same value. The increase in the apparent thickness during the second Hacac dose is, therefore, smaller than the increase during the first dose, which suggests that the inhibitor fragments on the surface are hindering the reapplication of Hacac inhibitor molecules. The apparent thickness measured after each O_2 plasma exposure appears to increase slightly with respect to the previous plasma exposure, which is corroborated by the IR data in Fig. S3 (Ref. 46) discussed later. Therefore, there seems to be a build-up of inhibitor fragments on the surface as a function of repeated removal and reapplication of inhibitor molecules. This build-up suggests that a part of the persisting species remains on the Al_2O_3 surface even after several O_2 plasma exposures. The O_2 plasma, therefore, does not seem to fully satisfy the requirements for area-selective ALD with a plasma coreactant as discussed in the Introduction.

Alternatively, an H_2 plasma could be employed to remove the acac adsorbates. H_2 plasma has been reported to be very effective at removing acac adsorbates during atomic layer etching (ALE) of AlN using $Sn(acac)_2$.[35] The removal of acac inhibitor species with an H_2 plasma was investigated using ellipsometry as shown in Fig. 2(c). The results suggest that, in contrast to an O_2 plasma, an H_2 plasma is able to completely remove the acac species from the surface, resulting in a clean Al_2O_3 surface. Moreover, the apparent thickness after each H_2 plasma exposure is slightly negative, indicating that the Al_2O_3 surface is altered or etched. Hacac has been reported to be a suitable reactant for ALE of Al_2O_3 at 250 °C.[36] In our process, repeated Hacac and H_2 plasma exposures were found to etch the Al_2O_3 slightly (with 0.0036 ± 0.0002 nm/cycle, see Fig. S2 in the supplementary material[46]), most likely through the formation of $Al(acac)_3$. The apparent thickness after each Hacac dose in Fig. 2(c) does not decrease as a result of this etching reaction, which indicates that it does not affect Hacac adsorption.

In order to investigate the persisting species in more detail, the removal of acac species by O_2 plasma was studied using IR spectroscopy. The results shown in Fig. 3 indicate that it is challenging to completely remove all adsorbed Hacac species from an Al_2O_3 substrate. No significant preference in the removal of Hacac in monodentate or chelate configuration[21] was observed during the O_2 plasma. Importantly, even after 100 s of O_2 plasma exposure, i.e., 20 times longer than what is normally used for the ABC-type process, C—O and C═O bond containing species persist on the surface, as can be seen in the spectra in Fig. 3(a). In addition, the different IR peaks attributed to adsorbed Hacac do not decrease with the same rates during the O_2 plasma exposure, as can be concluded from Fig. 3(b). The IR peaks that indicate the presence of C—O bond containing species decrease slower than the IR peaks attributed to C—C

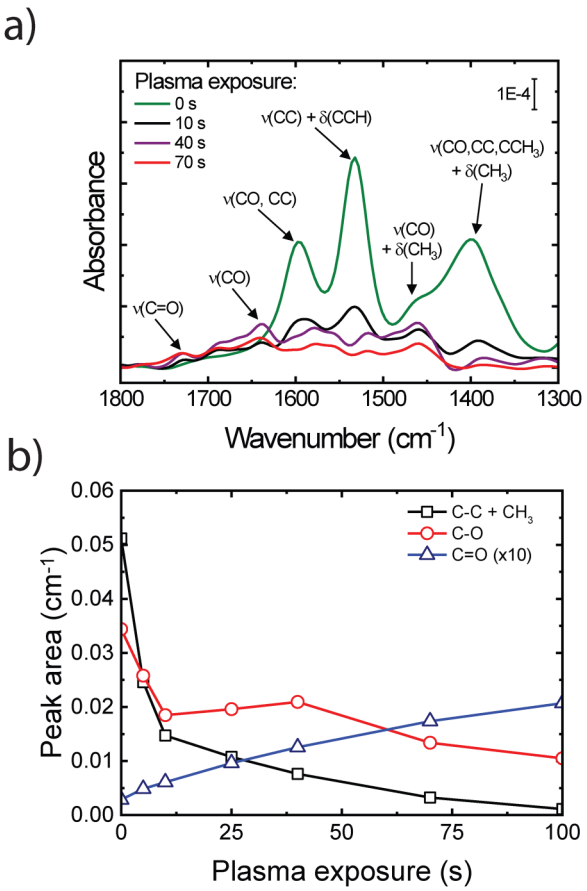

FIG. 3. (a) IR spectra of an Al_2O_3 substrate functionalized with Hacac, which has been exposed to O_2 plasma for different exposure times. The graph shows peak assignments that are based on the literature (Refs. 21, 37, and 38; see Table S1 in the supplementary material, Ref. 46). The skeletal deformation modes of the acac adsorbate complex are not included due to their relatively low intensities. (b) Integrated IR signal for C—C + CH_3 (1560 – 1500 + 1430 – 1320 cm^{-1}), C—O (1710 – 1560 + 1500 – 1430 cm^{-1}), and C═O (1775 – 1710 cm^{-1}) bond containing species as a function of O_2 plasma exposure. The integrated signal for the C═O bond containing species was multiplied by a factor of 10 for clarity. Note that there is an overlap between the IR adsorption of the CO and CC + CH_3 bond containing species, and therefore there is a small contribution of species containing C—O bonds to the integrated signal of the species containing C—C or CH_3 groups and vice versa. The integration ranges were chosen such that the effects of this overlap were mitigated.

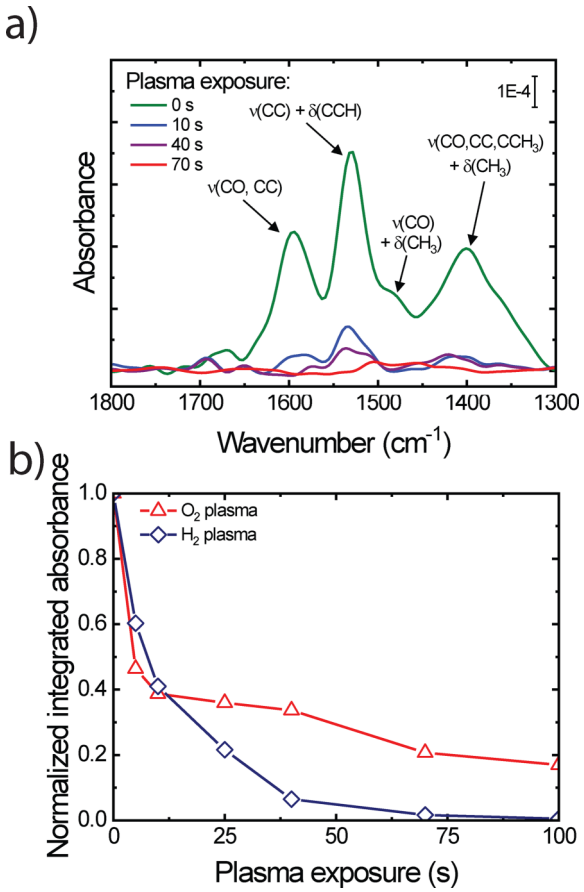

FIG. 4. (a) IR spectra of the Al_2O_3 substrate functionalized with Hacac during an H_2 plasma exposure. (b) Integrated IR signal of the Hacac spectra (1800 – 1300 cm^{-1}) as a function of O_2 and H_2 plasma exposure.

and C—H bond containing species. This observation suggests that the acac adsorbates are dissociated during the O_2 plasma exposure, resulting in inhibitor fragments on the surface. Moreover, the IR spectra show peaks at 1640 and 1730 cm^{-1} that increase with the O_2 plasma exposure, which indicates that new C—O and C═O bond containing species are formed on the Al_2O_3 surface during the removal reactions. Re-exposing the surface to Hacac after the O_2 plasma exposure (Fig. S3 in the supplementary material[46]) shows that these persisting C—O and C═O bond containing species hinder Hacac adsorption in the next cycle.

The persistence of Hacac fragments during the O_2 plasma is surprising at first sight as O_2 plasma is commonly used as the cleaning step to remove organics from a surface. However, the plasma conditions employed in this work are relatively mild and have, for example, been shown to allow for plasma-assisted ALD of SiO_2 on perovskite quantum dots without significant damage to the organic ligands of these quantum dots.[37] Note that, the formation of persisting C═O and C—O bond containing species, in the form of formates and carbonates, has also been reported during the O_2 plasma step of plasma-assisted ALD of Al_2O_3.[38–40] In the case of Al_2O_3 ALD, these formates and carbonates do not block precursor adsorption. The persisting acac fragments can be expected to behave similarly and could, therefore, lead to defects in the inhibitor layer as illustrated in Fig. 2(a). Possibly, complete Hacac removal could be achieved with harsher O_2 plasma conditions; however, the use of harsher O_2 plasma conditions is undesired as it could cause damage to the deposited SiO_2 layer or the employed substrate (e.g., carbon-doped SiO_2 and metal for FSAV applications).

Using an H_2 plasma was investigated as an alternative way of removing the acac adsorbates from the surface. In agreement with the ellipsometry results, the IR spectra in Fig. 4 show that complete acac removal can be achieved with an H_2 plasma. Moreover, in contrast to what was observed for an O_2 plasma, all the IR peaks attributed to acac adsorbates were found to decrease with the same trend (see Fig. S4 in the supplementary material[46]). Hacac adsorption after such an H_2 plasma exposure step should, therefore, be able to proceed independently from any previous inhibitor application or removal steps. The O_2 plasma step is still critical for the deposition of an SiO_2 film since greatly reduced and nonlinear growth was observed without the O_2 plasma step (see Fig. S5 in the supplementary material[46]), most likely due to incomplete removal of the precursor ligands. By employing H_2 and O_2 plasma exposures in a four-step ALD cycle, complete removal of both the inhibitor species and the precursor ligands can be achieved. The resulting ALD cycle, shown in Fig. 1, is referred to as an ABDC-type cycle such that labeling of the inhibitor, precursor, and O_2 plasma steps are the same as for the ABC-type cycle.

It is important to evaluate the material quality of the deposited material because it affects the insulating properties of the SiO_2 (e.g., C impurities typically result in a lower κ-value, whereas H impurities lead to a lower breakdown voltage).[41,42] In a previous work, SiO_2 layers grown with the BC-type process were electrically characterized and found to have a κ-value of 4.7.[43] Films deposited using BC-, ABC-, and ABDC-type cycles were characterized using IR spectroscopy (Fig. 5) and XPS depth profiling (Fig. S7 in the supplementary material[46]) in terms of impurities. The results show that no C impurities are incorporated for any of the ALD processes, which means that the material quality is not affected by dosing Hacac during ALD. In addition, no significant differences in the O content ($O/Si = 2.22 \pm 0.04$ for BC- and ABC-type cycles, and 2.17 ± 0.04 for ABDC-type cycles) were observed, which shows that the stoichiometry of the deposited SiO_2 is not affected. The IR spectra indicate that the H_2 plasma of the ABDC-type cycles results in a decrease of incorporated OH groups with respect to the other processes, whereas the number of incorporated SiH groups is increased. However, after a 450 °C anneal in an N_2 environment (i.e., BEOL compatible), it was found that those SiH and SiOH groups could be removed from the ABDC-type grown SiO_2 films (see Fig. S6 in the supplementary material[46]). These results, therefore, show that similarly high-quality SiO_2 films can be obtained using the BC- and ABDC-type ALD processes.

Nucleation curves for BC-, ABC-, and ABDC-type ALD cycles were measured using ellipsometry in order to investigate the effects of the added H_2 plasma step on the ALD growth. SiO_2 ALD was found to result in immediate growth on an SiO_2 substrate regardless of which an ALD cycle was employed as shown in Fig. 6(a). Moreover, no significant differences in the growth per cycle were observed between the studied processes, meaning that the growth of SiO_2 is not affected by the H_2 plasma. In contrast, the addition of the H_2 plasma step does have an influence on the nucleation of

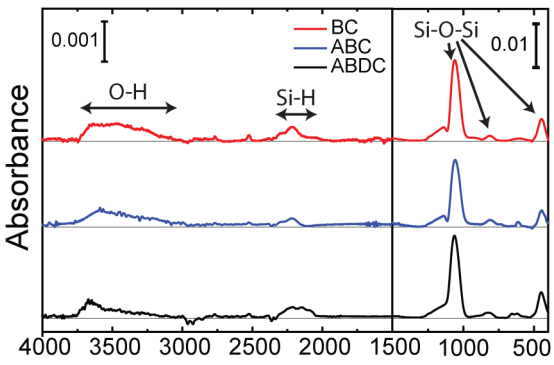

FIG. 5. (a) *Ex situ* IR spectra of SiO_2 layers deposited using 100 BC, ABC, or ABDC-type ALD cycles.

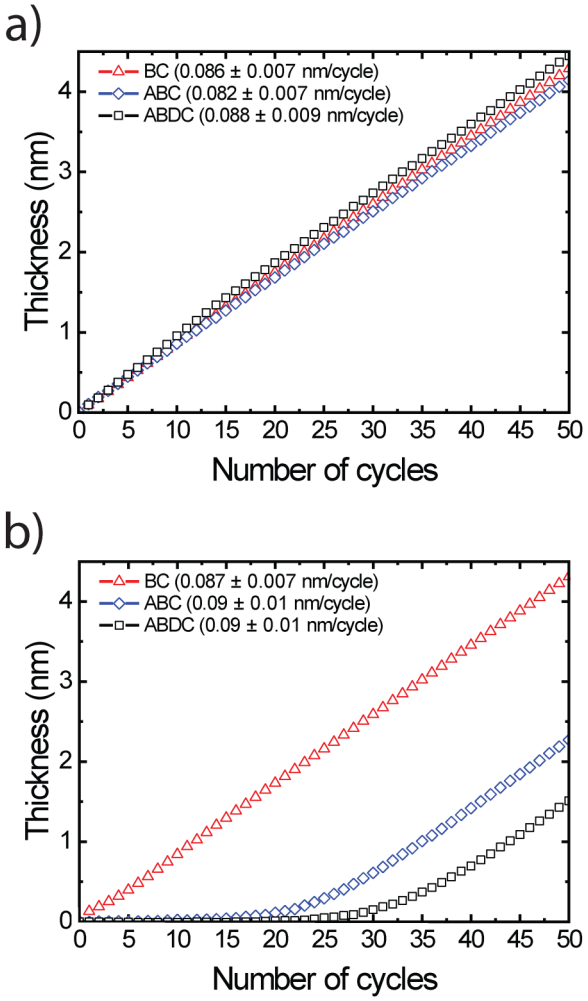

FIG. 6. Nucleation curves as measured by *in situ* ellipsometry for the BC, ABC, and ABDC-type ALD processes on (a) SiO_2 substrates and (b) Al_2O_3 substrates. The growth per cycle of each process in the linear growth regime of the nucleation curves is listed in the legends of (a) and (b).

SiO_2 ALD on Al_2O_3 surfaces, as shown in Fig. 6(b). As expected from our previous work,[20] SiO_2 nucleates readily on an Al_2O_3 substrate when the BC-type ALD process is employed, whereas adding an Hacac inhibitor dose to the ALD process results in a nucleation delay of 18 ± 2 ALD cycles (defined as the cycle after which the selectivity drops below 0.9).[44,45] This nucleation delay was found to be reproducible with a minimal run-to-run variability (see Fig. S8 in the supplementary material).[46] Importantly, the nucleation delay can be extended to 30 ± 3 cycles by adding an H_2 plasma step, which is attributed to the more complete removal of the adsorbed inhibitor species at the end of each cycle, as described above. As a result, the ABDC-type ALD cycle is able to deposit 2.7 ± 0.3 nm SiO_2 (with a selectivity of 0.9),[44,45] whereas the ABC-type ALD process was only capable of depositing 1.6 ± 0.2 nm.

IV. CONCLUSIONS

The removal of inhibitor species during area-selective ALD using a plasma was investigated in terms of the mechanisms that can affect the selectivity. It was found that an O_2 plasma cannot completely remove all Hacac inhibitor species from an Al_2O_3 surface. The Hacac species that persist during the O_2 plasma exposure were found to consist of Hacac fragments. IR spectroscopy shows that C—O and C═O containing species are formed during the O_2 plasma exposure of the area-selective ALD process. These species do not effectively block precursor adsorption and, therefore, act as defects in the inhibitor layer during area-selective ALD. Alternatively, an H_2 plasma was observed to result in complete removal of inhibitor species, leaving a clean non-growth area for inhibitor adsorption in the next ALD cycle. The nucleation delay for area-selective ALD of SiO_2 was extended significantly by adding an H_2 plasma step to the ALD cycle before the O_2 plasma coreactant step.

The requirement of complete inhibitor removal during the process can be generalized to other area-selective ALD approaches. When using a highly reactive coreactant, it can be expected that dissociation of the inhibitor takes place during the coreactant exposure, and therefore it is vital that the inhibitor molecules are completely removed before the next inhibitor dose. For ALD processes using ozone as coreactant, the formation of persisting formates and carbonates was also reported,[38] which suggests similar dissociation reactions can also be expected in area-selective ALD processes that involve ozone. When using SAMs as an inhibitor layer, the selectivity is often lost due to ALD growth within or on top of the SAM layer.[25] In this case, the removal of the SAM layer was shown to be very beneficial for the selectivity as this also allows for removal (i.e., lift-off) of the deposited material.[15,26] From the current study, we learn that reapplication of the inhibitor does not necessarily restore the inhibitor layer to its original state before degradation. The addition of a dedicated inhibitor removal step should, therefore, be considered to achieve area-selective ALD with high selectivity.

ACKNOWLEDGMENTS

This study was performed with the support of Lam Research Corp. The authors would like to thank Vincent Vandalon for the valuable discussions and Caspar van Bommel, Jeroen van Gerwen, Cristian van Helvoirt, Joris Meulendijks, and Janneke Zeebregts for the technical assistance.

DATA AVAILABILITY

The data that support the findings of this study are available within the article and its supplementary material.[46]

REFERENCES

[1]R. Clark, K. Tapily, K.-H. Yu, T. Hakamata, S. Consiglio, D. O'Meara, C. Wajda, J. Smith, and G. Leusink, APL Mater. **6**, 058203 (2018).
[2]B. Vincent, J.-H. Franke, A. Juncker, F. Lazzarino, G. Murdoch, S. Halder, and J. Ervin, Extrem. Ultrav. Lithogr. **IX10583**, 29 (2018).
[3]G. Murdoch, J. Bommels, C. J. Wilson, K. B. Gavan, Q. T. Le, Z. Tokei, and W. Clark, *2017 IEEE International Interconnect Technology Conference (IITC)*, Hsinchu, Taiwan (IEEE, New York, 2017), p. 1.
[4]A. J. M. Mackus and M. J. M. Merkx, AtomicLimits **7** (2019), see https://www.atomiclimits.com.
[5]J.-H. Franke, M. Gallagher, G. Murdoch, S. Halder, A. Juncker, and W. Clark, Proc. SPIE **10145**, 1014529 (2017).
[6]G. N. Parsons and R. D. Clark, Chem. Mater. **32**, 4920 (2020).
[7]A. J. M. Mackus, A. A. Bol, and W. M. M. Kessels, Nanoscale **6**, 10941 (2014).
[8]S. M. George, Chem. Rev. **110**, 111 (2010).
[9]J. Y. Choi, C. F. Ahles, R. Hung, N. Kim, and A. C. Kummel, Appl. Surf. Sci. **462**, 1008 (2018).
[10]X. Jiang, H. Wang, J. Qi, and B. G. Willis, J. Vac. Sci. Technol. A **32**, 041513 (2014).
[11]B. Kalanyan, P. C. Lemaire, S. E. Atanasov, M. J. Ritz, and G. N. Parsons, Chem. Mater. **28**, 117 (2016).
[12]X. Jiang and S. F. Bent, J. Phys. Chem. C **113**, 17613 (2009).
[13]L. Lecordier, S. Herregods, and S. Armini, J. Vac. Sci. Technol. A **36**, 031605 (2018).
[14]M. D. Sampson, J. D. Emery, M. J. Pellin, and A. B. F. Martinson, ACS Appl. Mater. Interfaces **9**, 33429 (2017).
[15]D. Bobb-Semple, K. L. Nardi, N. Draeger, D. M. Hausmann, and S. F. Bent, Chem. Mater. **31**, 1635 (2019).
[16]R. Chen and S. F. Bent, Adv. Mater. **18**, 1086 (2006).
[17]I. Zyulkov, V. Madhiwala, E. Voronina, M. Snelgrove, J. Bogan, R. O'Connor, S. De Gendt, and S. Armini, ACS Appl. Mater. Interfaces **12**, 4678 (2020).
[18]W. Lee, N. P. Dasgupta, O. Trejo, J.-R. Lee, J. Hwang, T. Usui, and F. B. Prinz, Langmuir **26**, 6845 (2010).
[19]A. Yanguas-Gil, J. A. Libera, and J. W. Elam, Chem. Mater. **25**, 4849 (2013).
[20]A. Mameli, M. J. M. Merkx, B. Karasulu, F. Roozeboom, W. M. M. Kessels, and A. J. M. Mackus, ACS Nano **11**, 9303 (2017).
[21]M. J. M. Merkx, T. E. Sandoval, D. M. Hausmann, W. M. M. Kessels, and A. J. M. Mackus, Chem. Mater. **32**, 3335 (2020).
[22]R. Khan *et al.*, Chem. Mater. **30**, 7603 (2018).
[23]J. R. Avila, E. J. DeMarco, J. D. Emery, O. K. Farha, M. J. Pellin, J. T. Hupp, and A. B. F. Martinson, ACS Appl. Mater. Interfaces **6**, 11891 (2014).
[24]N. Prathima, M. Harini, N. Rai, R. H. Chandrashekara, K. G. Ayappa, S. Sampath, and S. K. Biswas, Langmuir **21**, 2364 (2005).
[25]S. Seo *et al.*, ACS Appl. Mater. Interfaces **9**, 41607 (2017).
[26]F. S. Minaye Hashemi, C. Prasittichai, and S. F. Bent, ACS Nano **9**, 8710 (2015).
[27]W. L. Gladfelter, Chem. Mater. **5**, 1372 (1997).
[28]S. Balasubramanyam, M. J. M. Merkx, M. A. Verheijen, W. M. M. Kessels, A. J. M. Mackus, and A. A. Bol, ACS Mater. Lett. **2**, 511 (2020).
[29]M. J. M. Merkx, S. Vlaanderen, T. Faraz, M. A. Verheijen, W. M. M. Kessels, and A. J. M. Mackus, Chem. Mater. **32**, 7788 (2020).
[30]S. W. King, ECS J. Solid State Sci. Technol. **4**, N3029 (2015).
[31]H. C. M. Knoops, T. Faraz, K. Arts, and W. M. M. (Erwin) Kessels, J. Vac. Sci. Technol. A **37**, 030902 (2019).

[32]R. A. Ovanesyan, E. A. Filatova, S. D. Elliott, D. M. Hausmann, D. C. Smith, and S. Agarwal, J. Vac. Sci. Technol. A **37**, 060904 (2019).
[33]S. B. S. Heil, J. L. van Hemmen, C. J. Hodson, N. Singh, J. H. Klootwijk, F. Roozeboom, M. C. M. van de Sanden, and W. M. M. Kessels, J. Vac. Sci. Technol. A **25**, 1357 (2007).
[34]E. Langereis, S. B. S. Heil, H. C. M. Knoops, W. Keuning, M. C. M. van de Sanden, and W. M. M. Kessels, J. Phys. D Appl. Phys. **42**, 073001 (2009).
[35]N. R. Johnson, H. Sun, K. Sharma, and S. M. George, J. Vac. Sci. Technol. A **34**, 050603 (2016).
[36]A. Mameli, M. A. Verheijen, A. J. M. Mackus, W. M. M. Kessels, and F. Roozeboom, ACS Appl. Mater. Interfaces **10**, 38588 (2018).
[37]Y. Jing, M. J. M. Merkx, J. Cai, K. Cao, W. M. M. Kessels, A. J. M. Mackus, and R. Chen, ACS Appl. Mater. Interfaces **12**, 53519 (2020).
[38]V. R. Rai, V. Vandalon, and S. Agarwal, Langmuir **28**, 350 (2012).
[39]D. N. Goldstein, J. A. McCormick, and S. M. George, J. Phys. Chem. C **112**, 19530 (2008).
[40]J. Kwon, M. Dai, M. D. Halls, and Y. J. Chabal, Chem. Mater. **20**, 3248 (2008).
[41]K. Y. Yiang, W. J. Yoo, Q. Guo, and A. Krishnamoorthy, Appl. Phys. Lett. **83**, 524 (2003).
[42]J. Zemek, M. Závětová, and S. Koc, J. Non-Cryst. Solids **37**, 15 (1980).
[43]G. Dingemans, C. A. A. van Helvoirt, D. Pierreux, W. Keuning, and W. M. M. Kessels, J. Electrochem. Soc. **159**, H277 (2012).
[44]G. N. Parsons, J. Vac. Sci. Technol. A **37**, 020911 (2019).
[45]Please note that the reported nucleation delay for the ABC-type ALD process in this work (20 ALD cycles) deviates from the reported nucleation delay in our previous work (15 ALD cycles) (Ref. 20). The deviation is cause by this work defining the nucleation delay as the ALD cycle after which the selectivity decreases below 0.9, whereas in a previous work, it was defined as the ALD cycle where ellipsometry first showed deposition.
[46]See supplementary material at http://dx.doi.org/10.1116/6.0000652 for the details on the optimization of the H_2 plasma conditions, the etching of Al_2O_3 using Hacac/H_2 cycles, IR peak assignment and integration, the growth of ABD-type cycles, XPS depth profiles, sample annealing, and process reproducibility.